Supporting Information for "Improved observations of deep earthquake ruptures using machine learning "

Qibin Shi[1] and Marine A. Denolle[1]

[1]Department of Earth and Space Sciences, University of Washington

Contents of this file

1. Figure S1. Loss during the training.

2. Figure S2. Map view of the apparent stress and scaled duration of deep earthquakes.

3. Figure S3. Corner frequency with earthquake moment.

4. Figure S4. Geometrical configuration between source directivity and seismic ray.

5. Figure S5. Spectra of noisy and denoised P waves of an Mw5.5 deep event.

6. Figure S6. Stress drop against seismic moment at different depths.

7. Figure S7. Stress drop derived from the duration estimates.

8. Figure S8. Fall-off rate of model spectra and the inferred apparent stress.

9. Figure S9. Source parameters estimated using the noisy raw P waves.

10. Figure S10. Fracture energy and radiation efficiency using the AK135-f model.

11. Figure S11. The SNR (dB) improvement for the deep earthquakes in this analysis.

––––––––

Corresponding author: Q. Shi, Department of Earth and Space Sciences, University of Washington, 4000 15th Avenue NE, Seattle, WA 98195-1310, USA. (qibins@uw.edu)

June 23, 2023, 7:28pm

Additional Supporting Information (Files uploaded separately)

1. Tables S1 (uploaded as `Seismic_network_DOI_list.txt`). The Digital Object Identifiers (DOIs) of seismic networks were used in this study. The network codes and DOIs are obtained from the International Federation of Digital Seismograph Networks (FDSN).
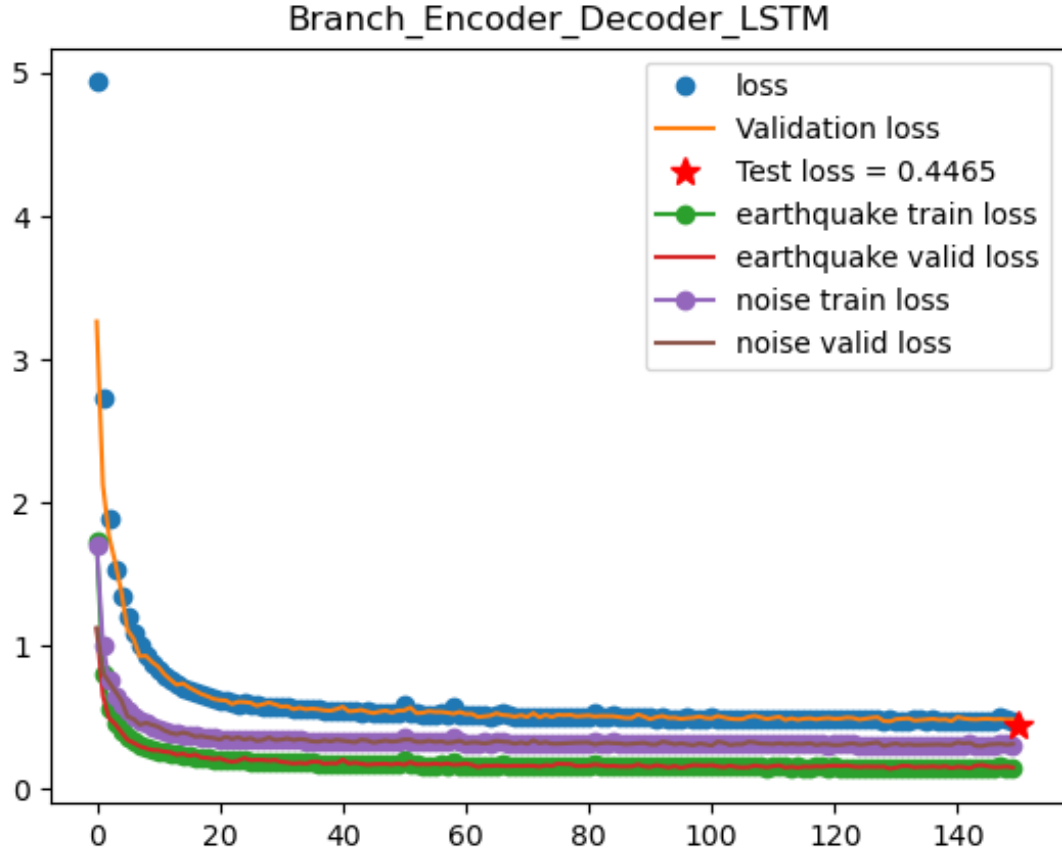
June 23, 2023, 7:28pm

Figure S1. Loss during the training. The loss of each reconstructed waveform is the average between the mean-squared error and the cross-correlation coefficient. The total loss (blue dots) is the sum of losses in the signal branch (green dots) and noise branch (purple dots). The validation loss is used to determine the termination time of the training in order to prevent overfitting.
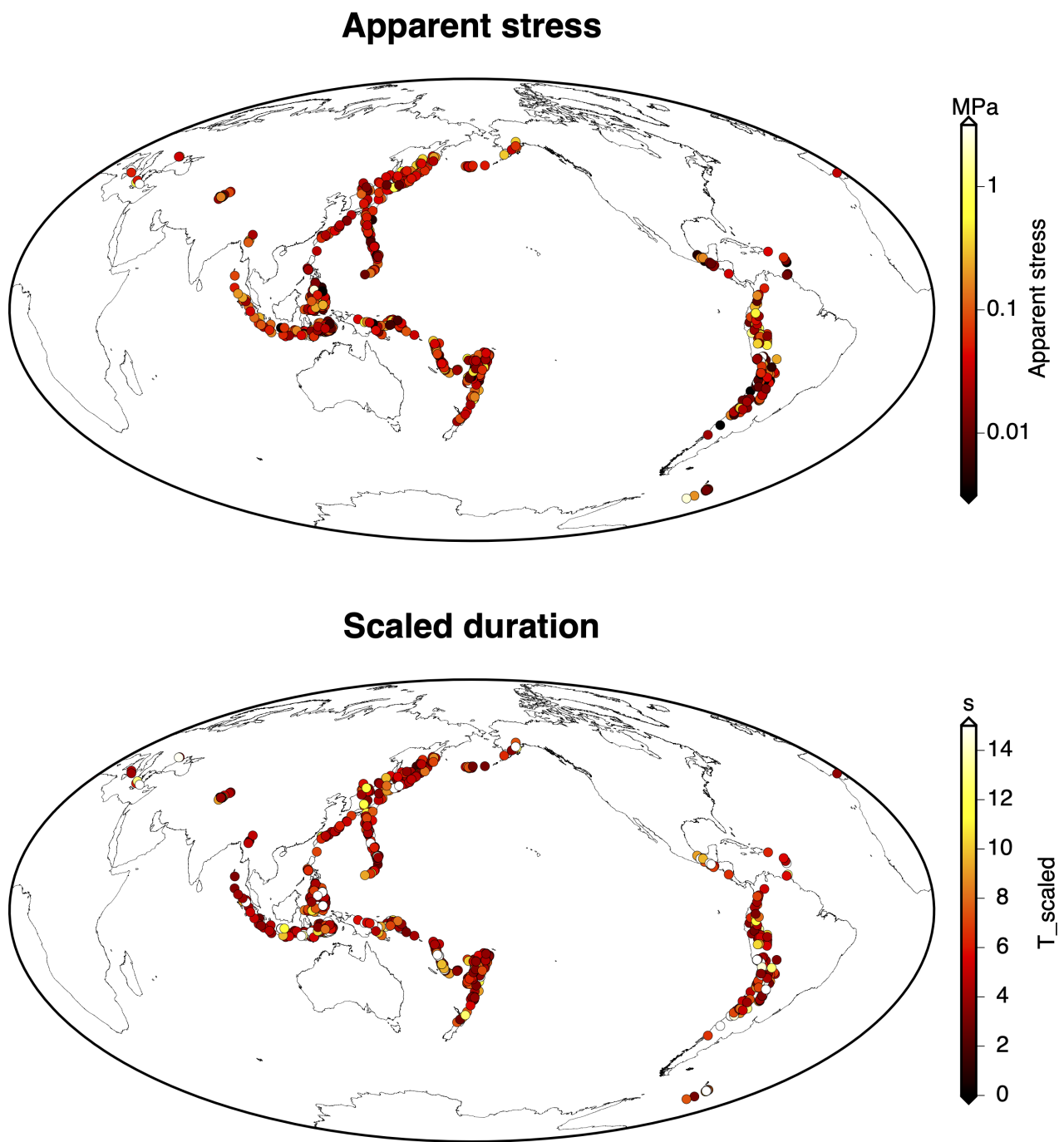
Apparent stress

Scaled duration

Figure S2. Map view of the apparent stress and scaled duration of the deep earthquakes.
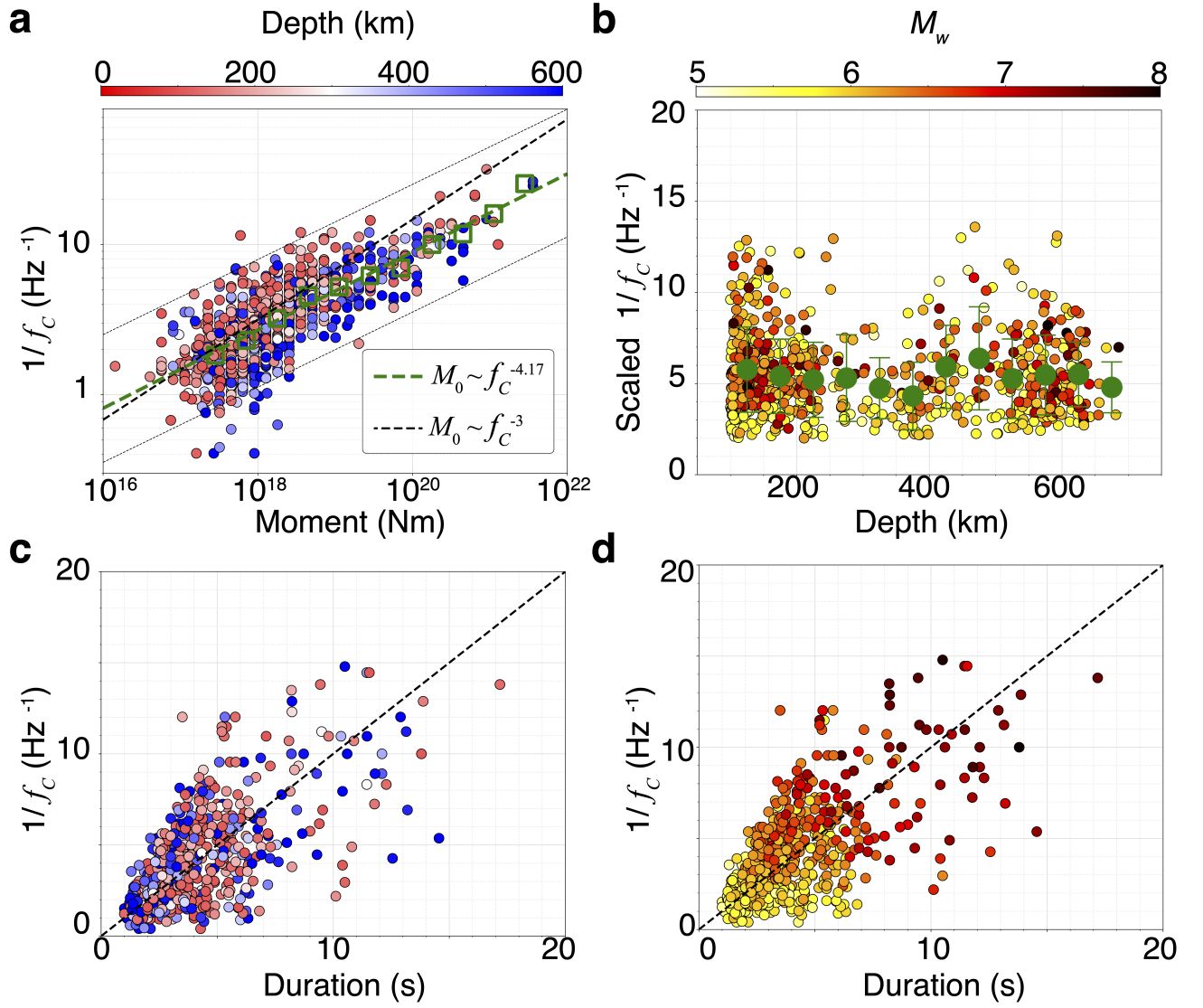
June 23, 2023, 7:28pm

Figure S3. Corner frequency with earthquake moment. (a) The scaling relation between the earthquake moment and the inverse of corner frequency is shown by dots color-coded by event depth and fitted with linear lines in the logarithmic space. (b) The inverse of corner frequency scaled to the same moment and shear-wave velocity is plotted with event depth. (c) and (d) show the same relation between the inverse of corner frequency and the source duration but color-coded by event depth and magnitude respectively.
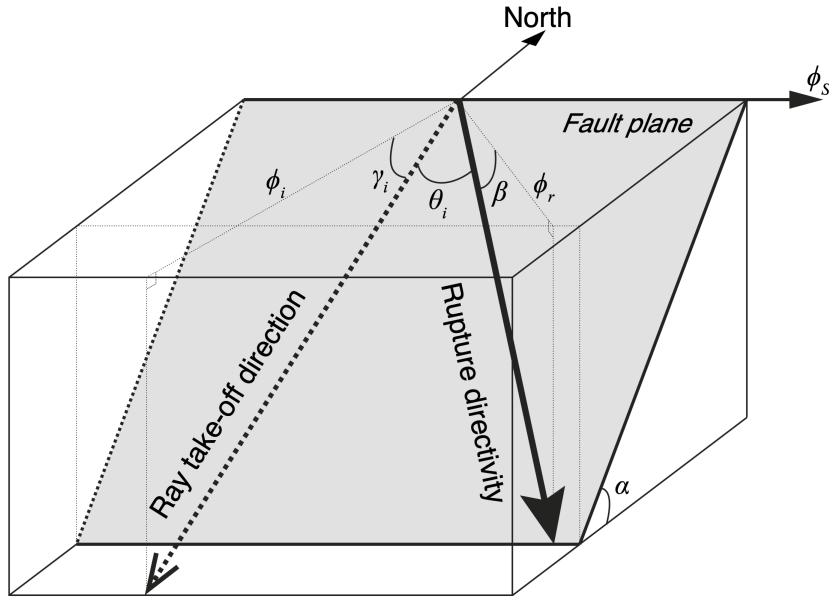
June 23, 2023, 7:28pm

Figure S4.   Cartoon representing the geometrical configuration between source directivity and seismic ray and the parameters used to calculate rupture directivity. The rupture direction is shown as a thick arrow with horizontal azimuth ϕ_r and inclination angle β is on the fault plane (shaded) with strike ϕ_S and dip α. The seismic ray between the source and the receiver is a dashed arrow with horizontal azimuth ϕ_i, and inclination angle γ_i deviates from the rupture directivity vector with an angle θ_i.
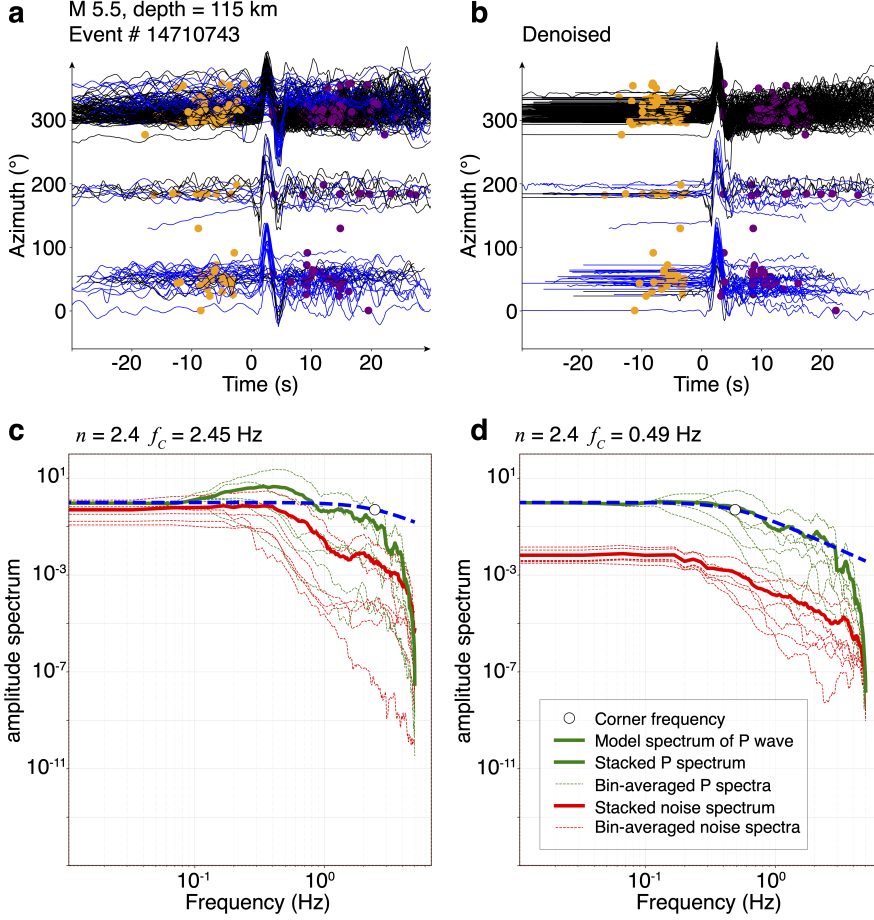
Figure S5. Spectra of noisy and denoised P waves of an Mw5.5 deep event. (a) and (b) are the raw P waves and the denoised P waves, respectively, of the Mw5.5 earthquake. The P waves are aligned with the peak amplitude, stretched based on the maximum cross-correlation coefficients and arranged by their station azimuth relative to the epicenter. The blue traces are flipped with signs for better alignment. The orange and purple dots mark the first and last points of the original time window for alignment. (c) and (d) are azimuthally binned average spectra and the stacked total spectra for noisy and denoised waveforms respectively. The thick green and red lines are the stacked spectra of the signal window and the noise window preceding the signal, respectively. The blue dashed lines are the best-fit spectral model, marked with the corner frequency shown as white dots.
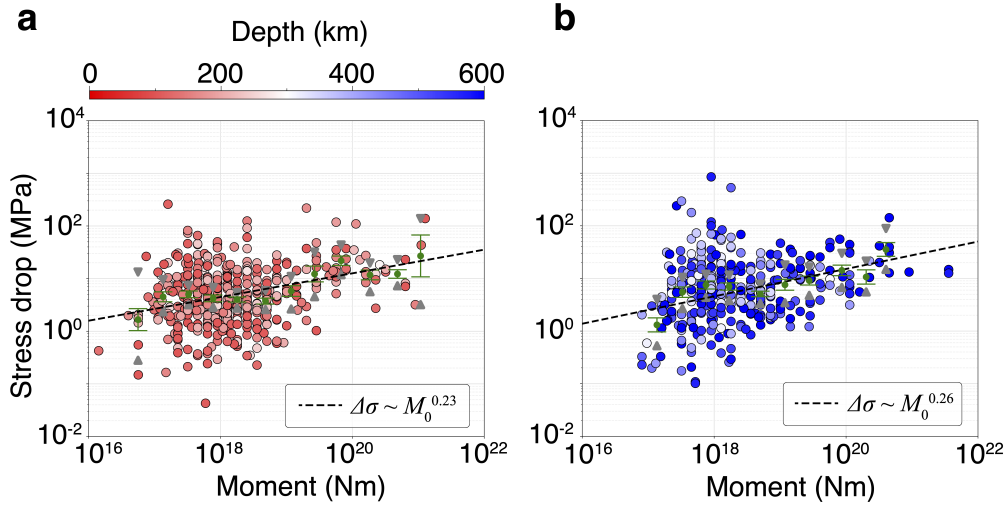
Figure S6. Stress drop against seismic moment in the two depth range: 100-300 km and 300-700km. The slope of the best fit regression is indicated in the text box.
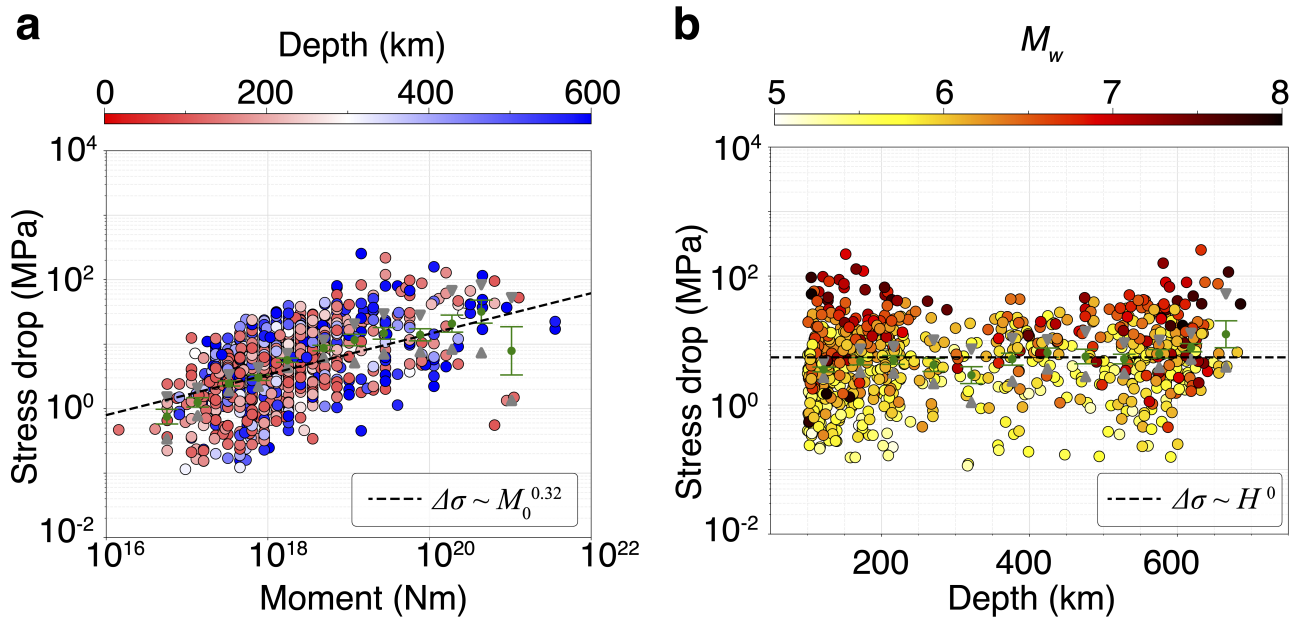

Figure S7. Stress drop derived from the duration estimates. (a) Stress drop against the seismic moment color-coded by depth. (b) Stress against depth color-coded by moment magnitude.
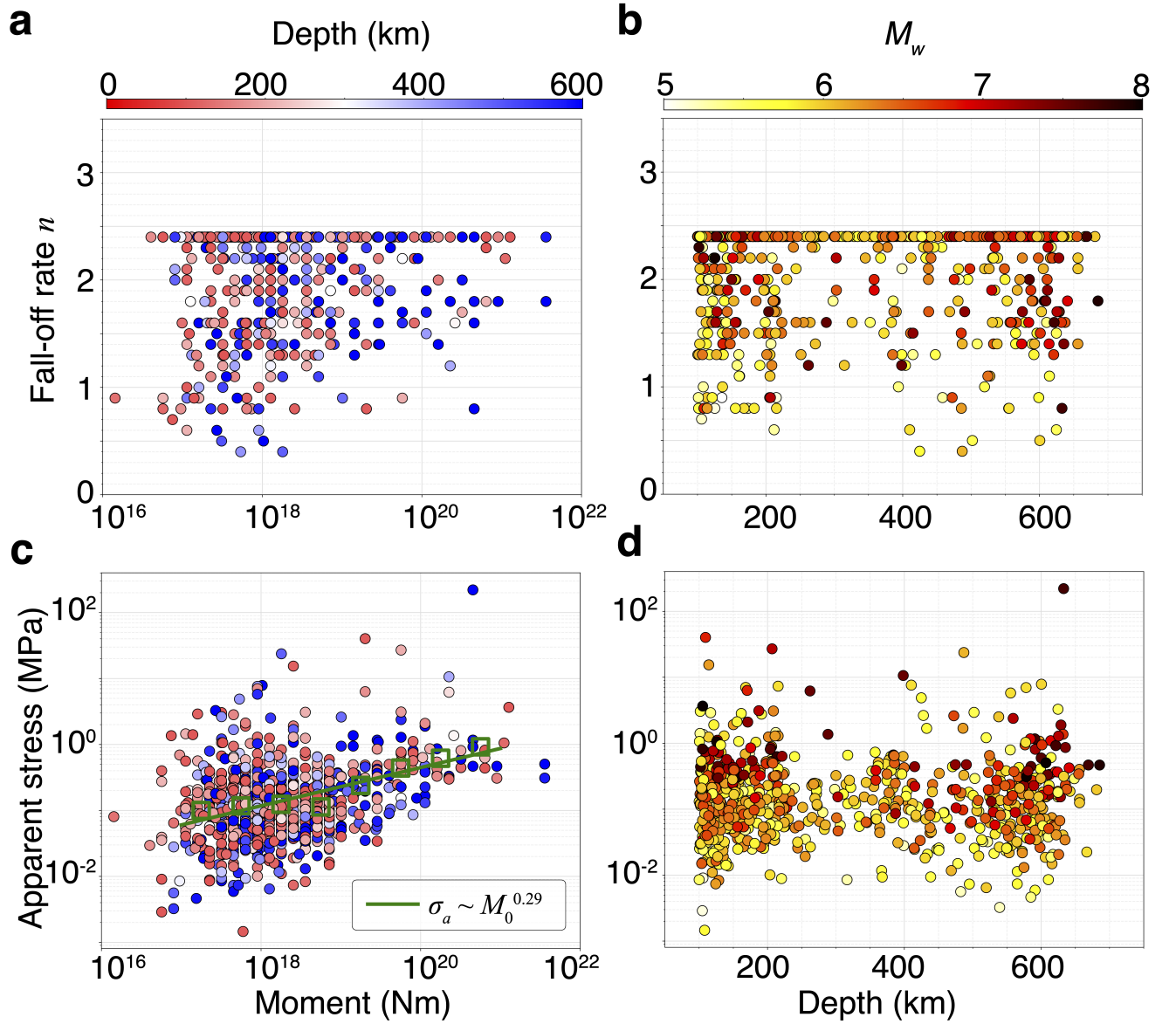
Figure S8. Fall-off rate of model spectra and the inferred apparent stress. (a) Variation of fall-off rate with earthquake moment color-coded by event depth. (b) Variation of fall-off rate with event depth color-coded by event size. (c) The scaling relation between the apparent stress and earthquake moment is color-coded by event depth. The green squares and the green line represent the binned average of apparent stress and the best-fit scaling relation. (d) Variation of apparent stress with event depth color-coded by event size.
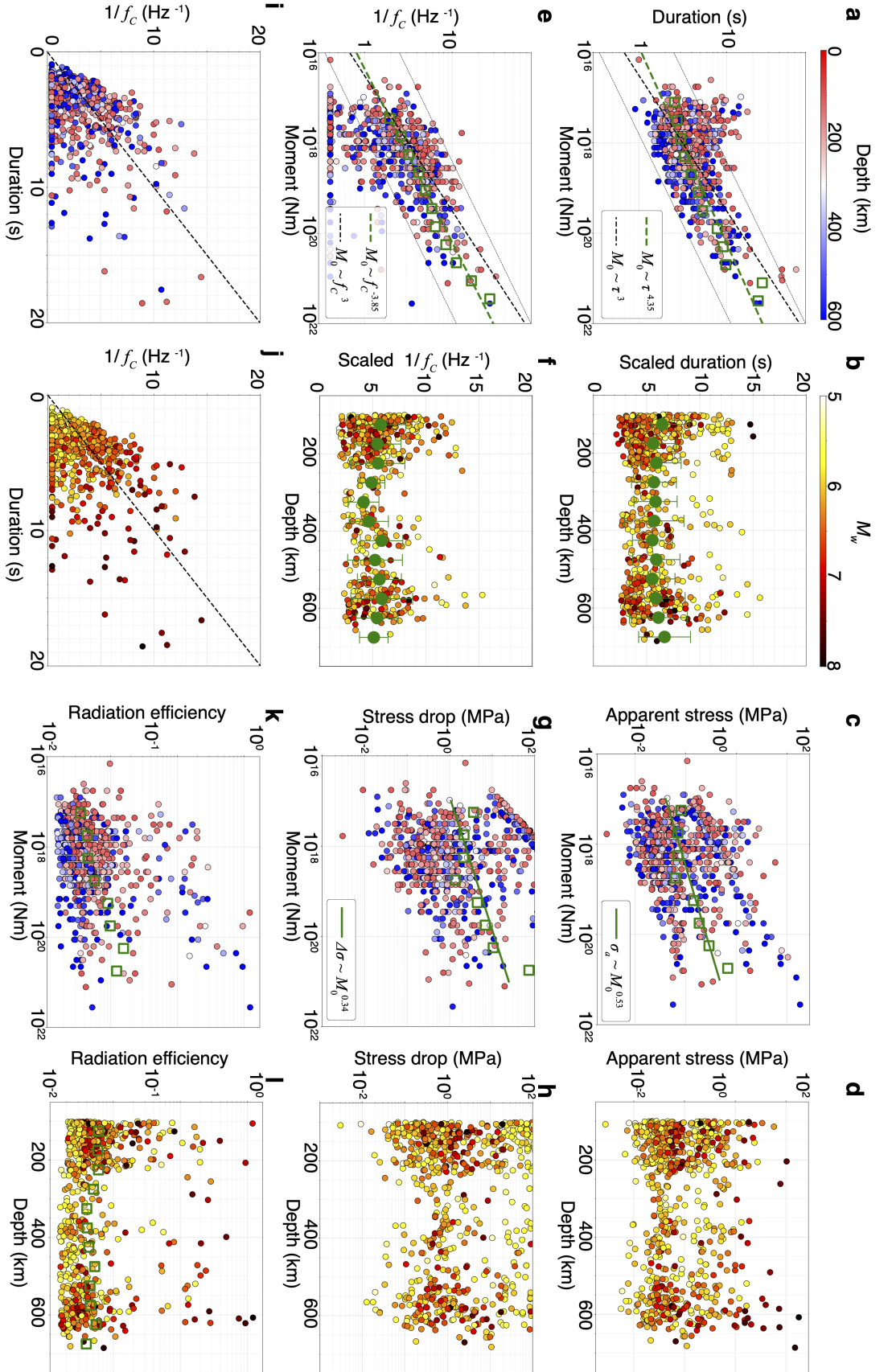
Figure S9. Source parameters estimated using the noisy raw P waves. The magnitude- and depth-dependence of source duration (a, b), corner frequency (e, f), apparent stress (c, d), stress drop (g, h), and radiation efficiency (k, l) present relatively larger uncertainties using the noisy P waves. The consistency between the temporal measurement of source duration and spectral-fitting derived corner frequency is relatively low compared to the denoised results.
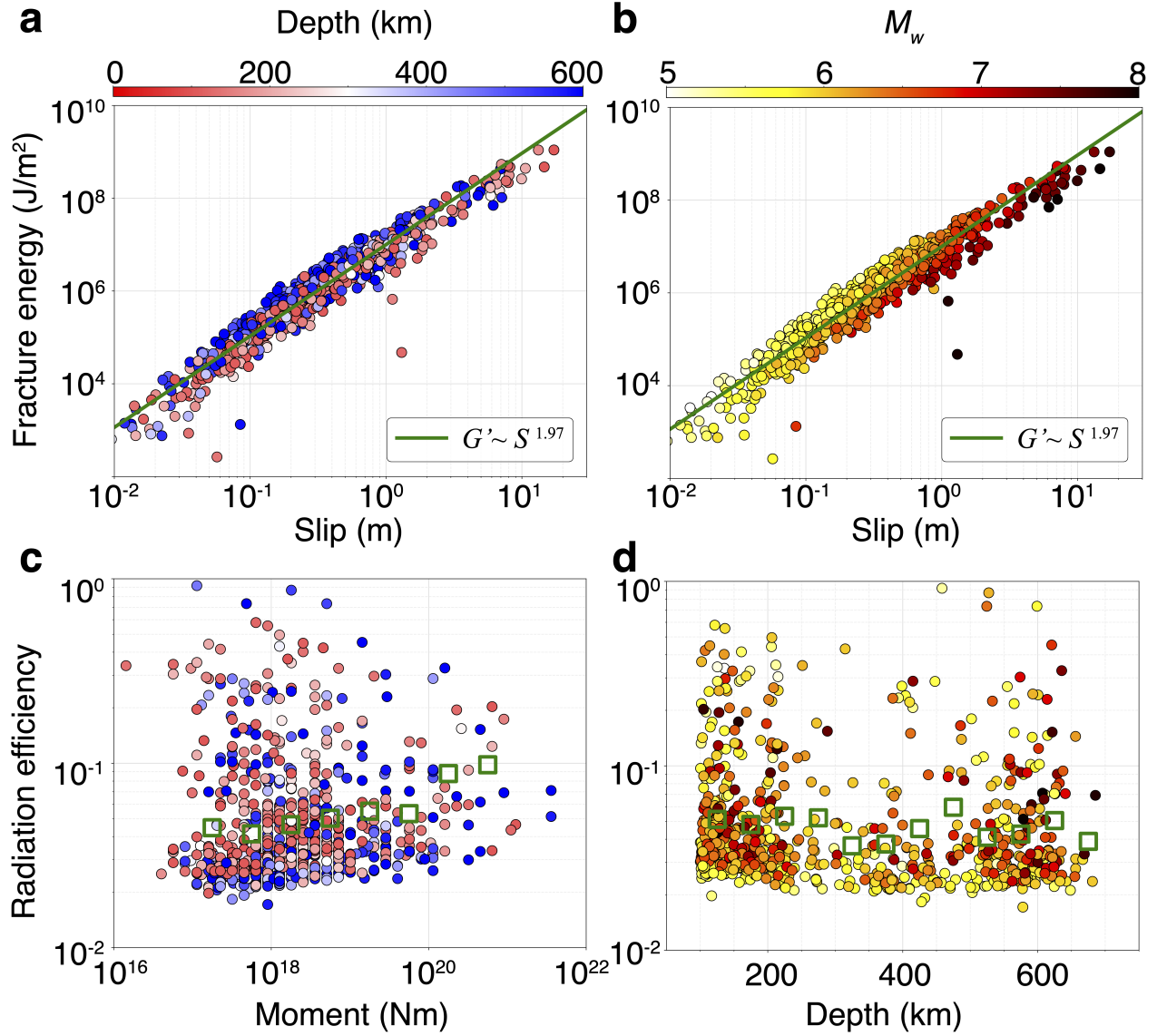
Figure S10. Fracture energy and radiation efficiency inferred using the AK135-f average Earth's velocity model. (a) and (b) are the scaling relation between fracture energy and slip that is best fitted by the power-law scaling. (a) is color-coded by event depth and (b) by event size. (c) Variation of radiation efficiency with earthquake moment. (d) Variation of radiation efficiency with teh event depth. Green squares represent the binned average values of radiation efficiency.
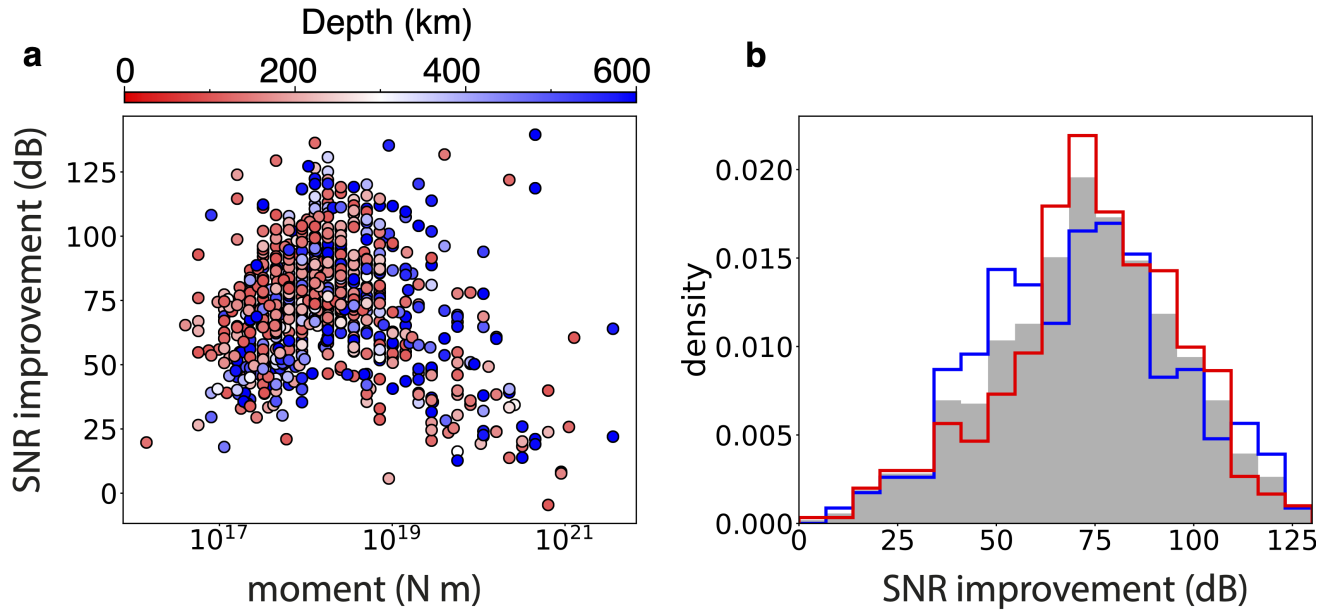
Figure S11.   The SNR (dB) improvement for the deep earthquakes in this analysis. (a) The average increase amount of SNR for individual events after denoising, shown against event moment color-coded by depth. (b) Histogram of the SNR improvement among all events selected for analysis.